Indonesian Journal of Science & Technology

Journal homepage: http://ejournal.upi.edu/index.php/ijost/

Innovative Nanofluid Encapsulation in Solar Stills: Boosting Water Yield and Efficiency under Extreme Climate Supporting Sustainable Development Goals (SDGs)

Tedjani Yahia Namoussa[1,], Leila Boucerredj[2], Abderrahmane Khechekhouche[1], Imad Kemerchou[3], Nadjet Zair[1], Mehdi Jahangiri[4], Abdelmonem Miloudi[1], Antonio Siqueira[5]*

[1]University of El Oued, El Oued, Algeria
[2]University of Guelma, Guelma, Algeria
[3]University of Ouargla, Ouargla, Algeria
[4]ShK.C., Islamic Azad University, Shahrekord, Iran
[5]University of Federal de Viçosa, Viçosa, Brazil
[*]Correspondence: E-mail: namoussa-tedjaniyahya@univ-eloued.dz

ABSTRACT

Water scarcity in extreme climates presents a global challenge directly linked to Sustainable Development Goals (SDGs), particularly SDG 6 (Clean Water and Sanitation). This study introduces an innovative solar still design using nanofluid encapsulation to enhance freshwater production because conventional systems often struggle with limited efficiency. The modified solar still employed sealed glass tubes containing CuO nanofluid, improving solar energy absorption and heat retention because the nanofluid could enhance thermal conductivity. The system maintained higher operational temperatures, leading to increased evaporation and freshwater yield. The encapsulation prevented nanoparticle contamination, ensuring water safety and long-term system stability. This approach demonstrates significant potential to support sustainable freshwater solutions aligned with global SDG targets under harsh environmental conditions.

© 2025 Tim Pengembang Jurnal UPI

ARTICLE INFO

Article History:
Submitted/Received 26 Mar 2025
First Revised 30 Apr 2025
Accepted 03 Jun 2025
First Available Online 04 Jun 2025
Publication Date 01 Dec 2025

Keyword:
Accumulated yield,
Efficiency,
Freshwater productivity,
Thermal performance,
Water temperature.

1. INTRODUCTION

In recent years, addressing water scarcity has become a global priority closely linked to the United Nations Sustainable Development Goals (SDGs), particularly SDG 6, which targets universal access to clean water and sanitation. In many arid and semi-arid regions, such as southeastern Algeria, groundwater frequently contains high salinity and mineral concentrations that exceed World Health Organization (WHO) standards, creating a critical challenge for clean drinking water access. Conventional water purification technologies often face economic, environmental, and energy-related limitations. Solar distillation has emerged as a promising, eco-friendly, and cost-effective technique for water purification because it sustainably utilizes abundant solar energy to produce potable water, even from industrial wastewater. However, its relatively low productivity remains a barrier to large-scale application, limiting widespread adoption. Therefore, extensive research has focused on improving the efficiency of solar stills through design innovations, material enhancements, and thermal optimization strategies to support progress toward SDG 6, as well as related goals such as SDG 7 (Affordable and Clean Energy) and SDG 13 (Climate Action). Numerous studies have explored modifications to solar still geometry and construction to enhance performance. For instance, thinner glass covers (3 mm) have proven more effective than thicker ones (5 or 6 mm), yielding higher productivity and energy efficiency [1]. Seasonal optimization of glass tilt angles between 20° and 30° has also shown performance improvements [2], while the use of double glazing (despite its success in other solar applications) resulted in significant productivity losses of up to 88.63% due to inhibited heat transfer [3-5].

Material-based interventions have also been widely studied. Incorporating locally available or recycled metallic or plant-based materials such as black zinc plates [6], palm fibers as the region has a large number of bearings [7, 8], aluminum waste from workshops [9], charcoal from waste burned by farmers [10], industrial coal debris [11], and palm stems have led to significant productivity gains, ranging from 8% to over 53% [12]. The same goes for rubber, Cladium mariscus, which is very abundant in the Sahara of the El Oued region, and the same goes for date kernels and Cellulose cardboard, which have been selected for their conductivity or high thermal absorption capacity, improve heat retention, and prolong the evaporation process [13-15].

Environmental and operational parameters also significantly affect solar still performance. Enhancements such as the addition of reflectors (mirrors) increased productivity by up to 45% [16], while optimized water depths (e.g., 1 cm) and thermal insulation strategies reduced basin losses and accelerated evaporation. Structural improvements like coupling the system with a heat storage tank enabled night time operation, boosting daily output by 27.7% and maintaining stable thermal efficiency in the absence of sunlight [17].

Other approaches have evaluated the use of natural materials such as local sand from El Oued and Illizi, with mixed results, ranging from decreased productivity to marginal improvements [18]. However, some materials have proven counterproductive: for example, plastic fins reduced system efficiency by nearly 9%, even absorbent multilayer composite materials [19, 20]. Another factor that reduces output is when solar radiation is low in the winter months [3, 19].

In terms of structural advancements, significant improvements in heat and mass transfer have been achieved using double-finned absorbers, solar concentrators, and alternative geometries such as conical, pyramidal, and tubular shapes, especially those with rotating absorbers, external reflectors, or pulsating heat pipes [21-24]. The condenser cooling system,

DOI: https://doi.org/10.17509/ijost.v10i3.85150
p- ISSN 2528-1410 e- ISSN 2527-8045

i.e., the glass cover, is a very effective method and has been used by several researchers [11]. Wick-type systems using materials like jute, particularly in rotating, inclined, or multi-condensing configurations, have demonstrated marked productivity gains and higher exergy efficiency, with improvements reaching up to 163% [25, 26].

A more recent and promising direction involves hybrid and material-based enhancements. Phase change materials (PCMs), when integrated into solar stills, have been shown to increase energy storage and thermal efficiency in both freshwater production and wastewater treatment contexts [27-29].

Finally, the integration of nanomaterials has introduced a transformative dimension to solar still design. The use of nanoparticles such as coal and graphene (either suspended in phase change matrices or stored in copper cylinders) has significantly improved thermal conductivity, leading to substantial enhancements in desalination efficiency [30]. Synergistic systems combining nanoparticles, PCMs, and nanocoatings have demonstrated exceptional gains, with reported productivity increases reaching up to 318% [31, 32]. These nano-enhanced configurations represent a cutting-edge approach to overcoming the performance limitations of conventional solar stills and offer a promising route toward high-efficiency, scalable water purification solutions.

This study examines the impact of a copper oxide (CuO) nanofluid, contained in strategically placed glass tubes, on the freshwater yield of a solar still. The main objective is to evaluate the effect of this specific nanofluid configuration on the distiller's efficiency. Innovations in this approach include the encapsulation of the CuO nanofluid in sealed glass tubes, thus preventing direct contamination of the pond water and ensuring the lasting effect of the nanomaterial throughout the distillation process. Furthermore, the organized arrangement of these nanofluid-filled tubes in the solar still basin represents another innovative aspect of this work, designed to maximize solar energy absorption and heat transfer to improve overall distillation efficiency. This method offers a distinct advantage by confining the nanofluid, thus mitigating potential losses and maintaining its concentration for prolonged performance improvement.

2. METHODS

2.1. Setup Experience

Figure 1. Figure 1 shows the experimental setup, consisting of two identical single-basin solar stills arranged side by side. Each is a rectangular enclosure with a transparent glass lid tilted to allow condensation and collection of distilled water. Inside each still, a series of glass tubes is visible, arranged in parallel and organized within the basin. We experimented on 23 March 2024, using these two solar stills of similar size and construction. The first, labeled "SSM" (modified solar still), was equipped with 15 glass tubes. These tubes were filled with an aqueous suspension containing 0.23% copper oxide (CuO) nanoparticles, which appears as a clear yellow-green liquid inside the tubes. The second still, labeled "CSS" (conventional solar still), served as a control. It was also equipped with 15 identical glass tubes, but these tubes were filled with pure, clear water, as shown in the inset at top left.

We verified that the glass tubes used in both stills were identical in terms of dimensions and material. This careful control allowed us to isolate the effect of the copper oxide nanoparticles present in the tubes, the only variable influencing the stills' performance. These solar stills were placed outdoors, in full sunlight, on a clear, windless day in Guemar, El Oued Province, Algeria. We began the experiment at 6:00 a.m. and continued until 4:00 p.m., recording measurements every hour. These measurements included the temperature of the

DOI: https://doi.org/10.17509/ijost.v10i3.85150
p- ISSN 2528-1410 e- ISSN 2527-8045

interior and exterior surfaces of the glass lid, the temperature of the water in each still's basin, and the cumulative amount of distilled water produced and collected in each still.

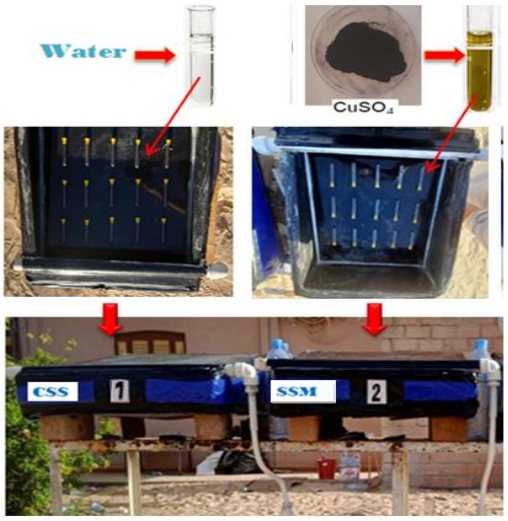

Figure 1. Experiment setup.

2.2. Energy Balance

The mathematical modeling of a single-slope solar still illustrates the various heat exchanges that occur in a solar still. It is based on four key points: glazing balance (energy interaction with the glass), water balance (energy changes in the water), insulation balance (heat management at the base), and condensate flow (freshwater production rate). Understanding these balances is essential for optimizing the design and operation of solar stills. It helps identify energy losses, determine the impact of design changes, and maximize freshwater production, thus improving the efficiency of solar stills as a viable solution for freshwater production, especially in regions where water is scarce. The equations are then delivered using symbols shown in **Table 1**.

Table 1. Nomenclature.

Symbol	Description	Unit
A_b	Surface area of the basin	m^2
C_{pb}	Specific heat of the bottom	J/(kg·K)
C_{pg}	Specific heat of the glass	J/(kg·K)
C_{pi}	Specific heat of the insulation	J/(kg·K)
C_{pw}	Specific heat of the water	J/(kg·K)
G	Solar radiation	W/m^2
G	Solar radiation	W/m^2
L	Latent heat of vaporization of water	J/kg
$\dot{m}_{ew}$	Mass of water evaporated	kg
M_b	Mass of the bottom	kg
M_g	Mass of the glass	kg
M_i	Mass of the insulation	kg
M_w	Mass of the water	kg
$Q_{c,b-i}$	Convective heat flow between the tank and the thermal insulation	W/m^2
$Q_{c,b-w}$	Convective heat flow between the bottom of the distiller and the water film	W/m^2
$Q_{c,g-a}$	Convective heat flow between the glass and the ambient	W/m^2
$Q_{c,ge-gi}$	Heat flows by conduction through the glass	W
$Q_{c,i-a}$	Convective heat flow between the insulation and the ambient	W/m^2

DOI: https://doi.org/10.17509/ijost.v10i3.85150
p- ISSN 2528-1410 e- ISSN 2527-8045

Table 1 (Continue). Nomenclature.

Symbol	Description	Unit
$Q_{c,w-gi}$	Convective heat flow between the water film and the glazing	W/m²
Q_{evap}	Evaporative-condensation heat flux between the water film and the glazing	W/m²
$Q_{r,g-a}$	Thermal radiation flux between the glass and the ambient	W/m²
$Q_{r,i-a}$	Radiative heat flow between the insulation and the ambient	W/m²
$Q_{r,w-gi}$	Thermal radiation flux between the water film and the glazing	W/m²
t	Time	s
T_b	Temperature of the bottom	K
T_{ge}	Temperature of the glass (outside)	K
T_{gi}	Temperature of the glass (inside)	K
T_i	Temperature of the insulation	K
T_w	Temperature of the water	K
α_b	Absorptivity of the bottom	dimensionless
α_g	Absorptivity of the glass	dimensionless
α_i	Absorptivity of the insulation	dimensionless
α_w	Absorptivity of the water	dimensionless
τ_g	Transmissivity of the glass	dimensionless
τ_w	Transmissivity of the water	dimensionless

All of these balances are known and used in this field [33].

(i) On the outside: The quantity of heat received by the glass is evacuated by the conductivity through the system (Equation (1) dan (2)):

$$\frac{M_g Cp_g}{A_g}\frac{dT_{ge}}{dt} = \alpha_g G + Q_{c.ge\_gi} - Q_{r.g.w\_a} - Q_{c.g.\_a} \quad (1)$$

(ii) On the inside: The explanation is shown in Equation (2):

$$\frac{M_g Cp_g}{A_g}\frac{dT_{gi}}{dt} = Q_{r.w\_gi} + Q_{c.w\_gi} + Q_{evap} - Q_{c.gi\_ge} \quad (2)$$

2.2.1. Water Balance

Figure 1 shows the exchange of heat between the body of water and the inside of the glass; the same amounts of heat are found by convection, radiation, and evaporation, respectively (Equation (3)).

$$\frac{M_w Cp_w}{A_w}\frac{dT_w}{dt} = \alpha_w \tau_g G + Q_{c.b.\_w} - Q_{c.w.\_g} - Q_{evap} - Q_{r.w.\_g.i} \quad (3)$$

2.2.2. Bottom Balance Sheet (The Absorber)

The bottom balance is represented by Equation (4):

$$\frac{M_b Cp_b}{A_b}\frac{dT_b}{dt} = \alpha_b \tau_g \tau_w G - Q_{c.b\_w} - Q_{c.b\_i} \quad (4)$$

2.2.3. Balance Sheet Insulation

We use thermal insulation to reduce heat loss from the solar distiller, to show the energy balance of insulation. Equation (5) represents this balance:

$$\frac{M_i}{A_i}\frac{C_{pi} dT_i}{dt} = \alpha_i \tau_g \tau_w \tau_b G + Q_{c.b\_i} - Q_{c.i\_a} - Q_{r.i\_a} \quad (5)$$

DOI: https://doi.org/10.17509/ijost.v10i3.85150
p- ISSN 2528-1410 e- ISSN 2527-8045

2.2.4. Thermal Efficiency Equation

The thermal efficiency (ηth) of the solar still can be calculated as (Equation (6)):

$$\eta_{th} = \frac{\sum \dot{m}_{ew} L}{\sum I(t) A_b \times 3600} \times 100 \quad (6)$$

3. RESULTS AND DISCUSSION

3.1. Solar Radiation and Ambient Temperature

Figure 2 illustrates the hourly variation of solar radiation (in W/m²) and ambient temperature (in °C) during the experimental period from 6:00 a.m. to 4:00 p.m. on 23 March 2023, in Guemar, El Oued Province, Algeria. Solar radiation is a very important factor in solar distillation. It is represented by the black line, starting weakly in the morning, increasing continuously until its peak of about 1,000 W/m² around 1:00 p.m., and then decreasing throughout the afternoon. The ambient temperature, represented by the red line, followed a similar evolution, but peaked a little later, reaching about 33°C between 3:00 p.m. and 4:00 p.m., when solar radiation had already begun to decline. These variations in solar energy and air temperature are important in understanding how the solar still worked that day, because sunlight fueled the process and the ambient temperature affected the amount of heat lost from the still.

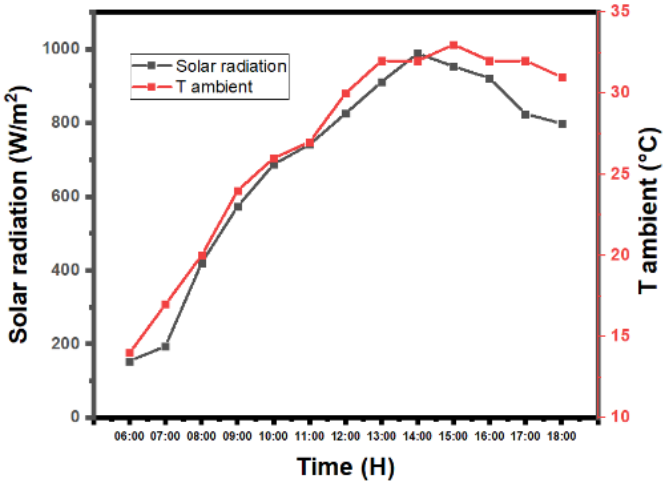

Figure 2. Radiation and ambient temperature.

3.2. Exterior Glass Temperature

Figure 3 illustrates the hourly variation in the outer glass temperature (°C) of the conventional solar still (CSS, black line with square marks) and the modified solar still (MSS, red line with circular marks) during the experimental period. Starting at approximately 14°C for the MSS and 13°C for the CSS at 6:00 a.m., the outer glass temperature of both stills gradually increased throughout the morning. By 11:00 a.m., the MSS reached approximately 39°C, while the CSS was approximately 36°C. Maximum temperatures were observed in the early afternoon, with the MSS reaching a maximum of approximately 45°C around 1:00 p.m. and the CSS slightly earlier, around 44°C around noon Notably, from about 10:00 a.m., the exterior glass temperature of the modified solar still (MSS) remained consistently 1-3°C higher than that of the CSS throughout the afternoon. With the decrease in solar radiation in the late afternoon, both temperatures decreased, reaching about 34°C for the MSS and 32°C for the CSS by 6:00 p.m. This consistently higher temperature in the MSS, especially during peak solar

DOI: https://doi.org/10.17509/ijost.v10i3.85150
p- ISSN 2528-1410 e- ISSN 2527-8045

hours, suggests that the modifications improve heat absorption and retention, leading to a warmer exterior glass surface than that of the control CSS. The overall temperature profiles reflect the influence of incident solar radiation and the improved heat transfer dynamics within the MSS.

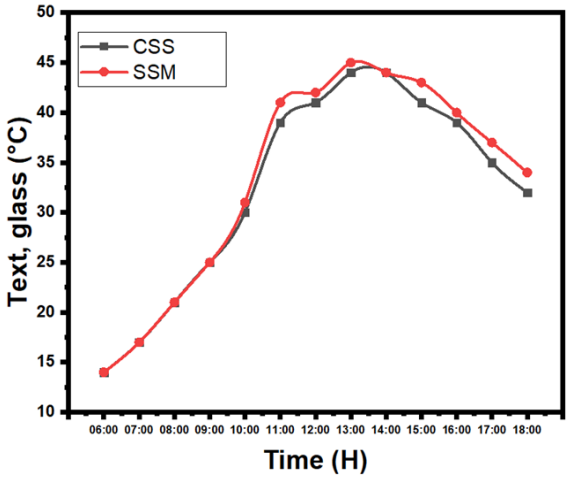

Figure 3. Outer glass temperature.

3.3. Interior Glass Temperature

Figure 4 illustrates the hourly variation of the inner glass temperature (°C) for both the conventional solar still during the experimental period. Starting at approximately 14°C for the MSS and 13.5°C for the CSS at 6:00 a.m., the inner glass temperature of both stills gradually increased throughout the morning. By 11:00 a.m., the MSS reached approximately 45°C, while the CSS was around 46°C. Maximum temperatures were observed in the mid-afternoon, with the MSS reaching a maximum of approximately 52°C around 3:00 p.m. and the CSS peaking slightly earlier at around 49°C around 2:00 p.m. Notably, from about 9:00 a.m. to 5:00 p.m., the inner glass temperature of the MSS generally remained 1 to 3°C higher than that of the CSS, with a more significant difference observed during the peak solar radiation hours in the afternoon. With the decrease in solar radiation in the late afternoon, both temperatures decreased, reaching about 44°C for the MSS and 42°C for the CSS by 6:00 p.m. This consistently higher inner glass temperature in the MSS during the majority of the day suggests that the modifications are effectively trapping more heat inside the still, leading to a warmer inner glass surface compared to the control CSS. The overall temperature profiles reflect the influence of incident solar radiation and the improved heat retention capabilities within the MSS.

3.4. Pond Water Temperature

Figure 5 illustrates the hourly variation of water temperature in a CSS without nanofluid and a MSS with nanofluid from 6:00 to 18:00 hours, showing that both experience a temperature increase due to solar radiation, with the most rapid rise between 8:00 a.m. and noon, followed by a slower increase likely due to heat loss. Notably, the MSS consistently maintained a higher water temperature throughout the day, starting at around 16°C compared to the CSS at 17°C, reaching peak temperatures of approximately 73°C for the MSS and 65°C for the CSS around 2:00 p.m., and remaining significantly warmer in the late afternoon at 51°C for the MSS versus 47°C for the CSS. This sustained higher temperature in the MSS indicates that the modifications, likely the use of nanofluids, enhance solar energy

DOI: https://doi.org/10.17509/ijost.v10i3.85150
p- ISSN 2528-1410 e- ISSN 2527-8045

absorption and heat transfer to the water, leading to more efficient heating compared to the conventional still, particularly during peak sunlight hours.

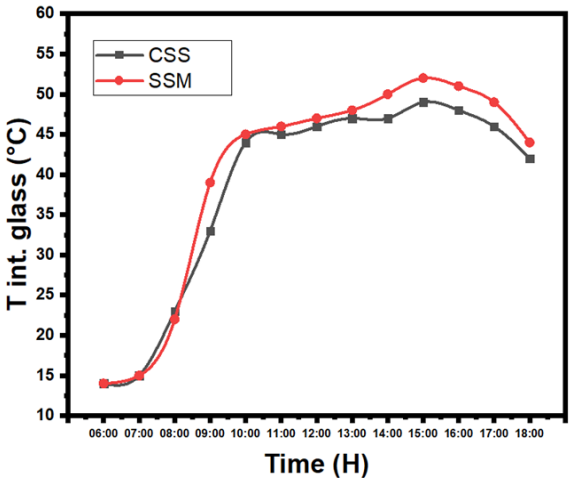

Figure 4. Inner glass temperature.

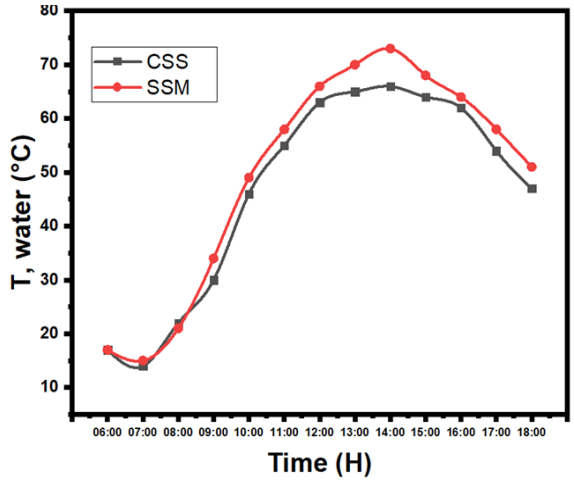

Figure 5. Water temperature variation.

3.5. Hourly Productivity

Figure 6 presents a bar chart illustrating the hourly flow rate (in mL) of freshwater produced by the conventional solar still (CSS, black bars) and the modified solar still (MSS, red bars). As illustrated, both stills exhibit minimal freshwater production in the early morning hours, with production beginning to increase significantly around 10:00 a.m., coinciding with the increase in solar radiation. The MSS consistently exhibits a higher hourly flow rate than the CSS throughout most of the day, particularly during the period of peak solar intensity, from early to mid-afternoon. The most significant difference in flow rate between the two stills is observed between 1:00 p.m. and 4:00 p.m., where the MSS exhibits significantly higher freshwater production, reaching a maximum flow rate of approximately 205 mL around 3:00 p.m., while the CSS peaks at approximately 120 mL around 2:00 p.m. This increased productivity of the MSS can be attributed to modifications made, including the incorporation of nanofluids that improve heat absorption and water evaporation. Even in the late afternoon, when solar radiation decreases, the MSS continues to produce a higher quantity of distilled water than the CSS. The cumulative effect of these hourly differences underlines the increased efficiency of the modified solar still in converting solar energy into fresh water

DOI: https://doi.org/10.17509/ijost.v10i3.85150
p- ISSN 2528-1410 e- ISSN 2527-8045

compared to the conventional design, under the same environmental conditions in Guemar, El Oued Province, Algeria.

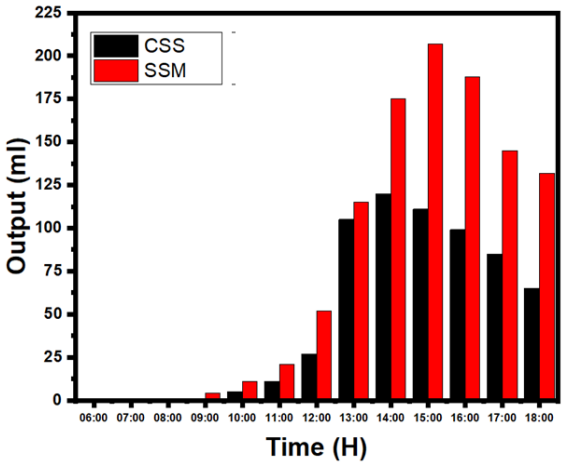

Figure 6. Hourly flow rate.

3.6. Accumulated Productivity

Figure 7 presents the cumulative productivity (in mL) of freshwater for the CSS and the MSS over the experimental period from 6 a.m. to 6 p.m. As expected, the cumulative production of both stills starts at zero in the early morning and gradually increases throughout the day. However, the MSS consistently exhibits a higher cumulative freshwater production rate than the CSS starting around 11 a.m. The gap in cumulative production becomes increasingly significant during the solar peak hours and continues into the late afternoon, highlighting the overall improved efficiency of the modified design. By the end of the experimental period at 6 p.m., the MSS achieves a significantly higher total cumulative freshwater production, reaching approximately 1,050 mL, while the CSS produces a total of approximately 630 mL. This represents an improvement of approximately 66.67% in the cumulative productivity of the MSS compared to the CSS during the experimental day. This substantial difference in cumulative production underlines the positive impact of the modifications made to the MSS, probably the use of nanofluids, by significantly comparing the total freshwater yield to that of the traditional solar still under the same environmental conditions in Guemar, El Oued province, Algeria, on 23 March 2023. The steeper slope of the MSS curve during most of the day visually represents its higher productivity over time.

3.7. Thermal Efficiency

Figure 8 illustrates the hourly variation in efficiency (%) for both solar stills. Both stills exhibit minimum efficiency in the early morning hours, with efficiency beginning to increase significantly around 10:00 AM. The MSS consistently demonstrates higher hourly efficiency than the CSS throughout most of the day, especially during the period of maximum solar intensity. The peak efficiency achieved by the MSS is approximately 57% around 3:00 p.m., while the peak efficiency of the CSS is approximately 32% around 2:00 p.m. The most significant difference in efficiency between the two stills is observed between 1:00 p.m. and 4:00 p.m. To quantify the improvement at the time of peak efficiency of the MSS, the improvement rate over the CSS is approximately 90%. Even at 6:00 p.m., the efficiency of the MSS (approximately 44%) remains significantly higher than that of the CSS (approximately 21%). Based on a visual estimate, the average efficiency over the experimental period is approximately 30–35% for MSS and 15–20% for CSS, suggesting an improvement of

DOI: https://doi.org/10.17509/ijost.v10i3.85150
p- ISSN 2528-1410 e- ISSN 2527-8045

approximately 85.7% in average efficiency due to the use of nanofluids in the modified still. This consistently higher efficiency and the overall MSS average indicate that the implemented modifications are more efficient in converting solar energy into freshwater production throughout the day, resulting in a significant performance improvement compared to the conventional design. The overall efficiency trends reflect the improved performance of the modified solar still in utilizing solar radiation for water distillation due to the inclusion of nanofluids.

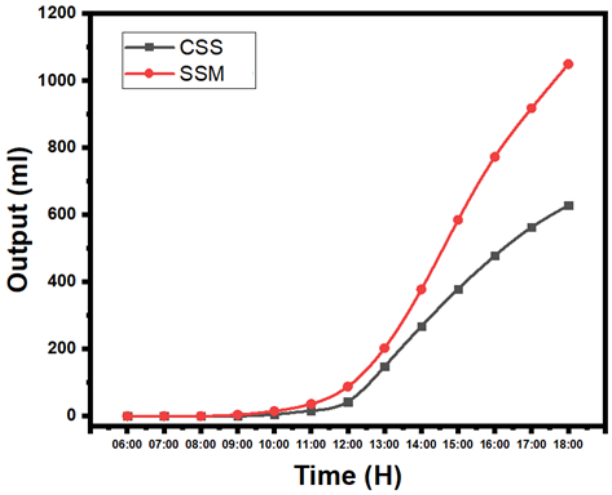

Figure 7. Cumulative productivity.

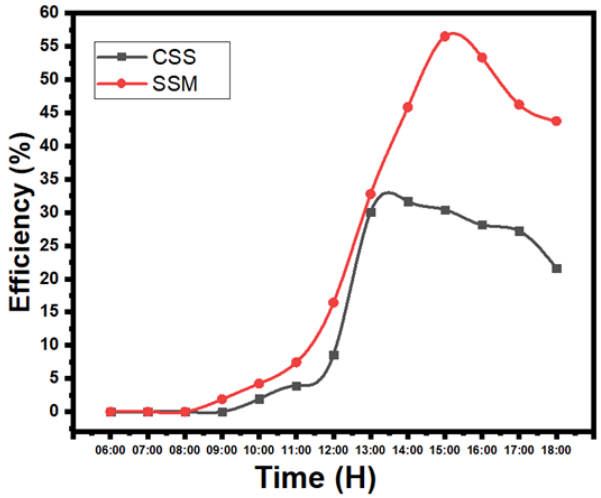

Figure 8. Thermal efficiency.

3.8. SDGs Contribution

The findings of this study directly contribute to the achievement of the United Nations SDGs, particularly SDG 6 (Clean Water and Sanitation), which emphasizes the importance of ensuring the availability and sustainable management of water for all. By enhancing the efficiency of solar stills through innovative nanofluid encapsulation, this research offers a sustainable solution for freshwater production in extreme climates where water scarcity is a major concern. The system utilizes abundant solar energy, promoting clean and renewable energy usage, thereby supporting SDG 7 (Affordable and Clean Energy). Additionally, by providing a low-cost, environmentally friendly, and scalable technology for decentralized water purification, the study indirectly contributes to SDG 13 (Climate Action) by reducing

DOI: https://doi.org/10.17509/ijost.v10i3.85150
p- ISSN 2528-1410 e- ISSN 2527-8045

reliance on fossil-fuel-based desalination methods. The integration of nanotechnology within a safe encapsulation framework ensures both environmental safety and long-term operational stability, aligning with the broader goals of sustainable development. This adds new information regarding SDGs as reported elsewhere [34-43].

4. CONCLUSION

The experimental results demonstrate the significant enhancement in freshwater productivity and efficiency achieved by the MSS compared to the CSS. The incorporation of modifications, likely involving nanofluids, led to consistently higher outer and inner glass temperatures, indicating improved solar energy absorption and heat retention within the MSS. Consequently, the water temperature in the MSS reached a peak of approximately 73°C, notably higher than the 65°C peak observed in the CSS. This resulted in a substantially greater accumulated freshwater yield of around 1050 mL for the MSS by the end of the day, representing an approximate 66.67% improvement over the CSS, which produced about 630 mL. Furthermore, the peak energy conversion efficiency of the MSS reached approximately 57%, significantly outperforming the CSS peak efficiency of around 32%, with an estimated average efficiency improvement of about 85.7%. These findings underscore the effectiveness of the implemented modifications in the MSS for enhancing solar distillation performance under the specific environmental conditions of the study.

5. AUTHORS' NOTE

The authors declare that there is no conflict of interest regarding the publication of this article. The authors confirmed that the paper was free of plagiarism.

6. REFERENCES

[1] Khechekhouche, A., Manokar, A. M., Sathyamurthy, R., Essa, F. A., Sadeghzadeh, M., and Issakhov, A. (2021). Energy, exergy analysis, and optimizations of collector cover thickness of a solar still in El Oued climate, Algeria. *International Journal of Photoenergy*, *2021*(1), 6668325.

[2] Cherraye, R., Bouchekima, B., Bouguettaia, H., Bechki, D., and Khechekhouche, A. (2020). The effect of tilt angle on solar still productivity at different seasons in arid conditions (South Algeria). *International Journal of Ambient Energy*, *43*(1), 1847-1853.

[3] Khechekhouche, A., Benhaoua, B., and Driss, Z. (2017). Solar distillation between a simple and double-glazing. *Recueil de Mécanique*, *2*(2), 145-150.

[4] Khechekhouche, A., Boubaker, B., Manokar, A. M., and Ravishankar, S. (2019). Dunes effect on the productivity of a single slope solar distiller. *Heat and Mass Transfer*, *56*(1), 1-10.

[5] Khechekhouche, A., Driss, Z., and Durakovic, B. (2019). Effect of heat flow via glazing on the productivity of a solar still. *International Journal of Energetica*, *4*(2), 54-57.

[6] Khechekhouche, A., Benhaoua, B., Kabeel, A. E., and Attia, M. E. H. (2019). Improvement of solar distiller productivity by a black metallic plate of zinc as a thermal storage material. *Journal of Testing and Evaluation*, *49*(2), 967-976.

DOI: https://doi.org/10.17509/ijost.v10i3.85150
p- ISSN 2528-1410 e- ISSN 2527-8045

[7] Kermerchou, I., Mahdjoubi, I., Kined, C., and Khechekhouche, A. (2022). Palm fibers effect on the performance of a conventional solar still. *ASEAN Journal for Science and Engineering in Materials*, *1*(1), 29-36.

[8] Miloudi, A., Khechekhouche, A., and Kermerchou, I. (2022). Polluted groundwater treatment by solar stills with palm fibers. *JP Journal of Heat and Mass Transfer*, *27*, 1-8.

[9] Bellila, A., Khechekhouche, A., Kermerchou, I., Sadoun, A., de Oliveira Siqueira, A. M., and Smakdji, N. (2022). Aluminum wastes effect on solar distillation. *ASEAN Journal for Science and Engineering in Materials*, *1*(2), 49-54.

[10] Sadoun, A., Khechekhouche, A., Kermerchou, I., Ghodbane, M., and (2022). Impact of natural charcoal blocks on the solar still output. *Heritage and Sustainable Development*, *4*(1), 61-66.

[11] Smakdji, N., Khechekhouche, A., Abdelgaied, M., Kabeel, A. E., Sadoun, A., and (2023). Energy and exergy investigation of industrial coal debris effect on solar still. *Environmental Progress and Sustainable Energy*, *42*(6), e14171.

[12] Kemerchou, I., Abderrahim, A., Khechekhouche, A., and Bellila, A. (2024). Enhancing solar still efficiency in Southeastern Algeria: An experimental case with palm stems. *Desalination and Water Treatment*, *317*, 100148.

[13] Aoun, Y., Chemsa, A., Khechekhouche, A., Bellila, A., Kermerchou, I., and (2023). Use of a local Saharan plant (Cladium mariscus) in the solar still under southeast Algeria climate. *Desalination and Water Treatment*, *311*, 162-168.

[14] Brihmat, A., Mahcene, H., Bechki, D., Bouguettaia, H., Khechekhouche, A., and Boughali, S. (2023). Energy performance improvement of a solar still system using date and olive kernels: Experimental study. *CLEAN – Soil, Air, Water*, *51*(2), 2200384.

[15] Bellila, A., Rahal, Z., Smolyanichenko, A., and Sadoun, A. (2023). Cellulose cardboard effect on the performance of a conventional solar still. *International Journal of Energetica, 8*(1), 44-49.

[16] Khechekhouche, A., Kabeel, A. E., Boubaker, B., and Attia, M. E. H. (2020). Traditional solar distiller improvement by a single external refractor under the climatic conditions of the El-Oued region, Algeria. *Desalination and Water Treatment*, *177*, 23-28.

[17] Khechekhouche, A., Smakdji, N., El Haj Assad, M., Kabeel, A. E., and Abdelgaied, M. (2023). Impact of solar energy and energy storage on a still's nocturnal output. *Journal of Testing and Evaluation*, *51*(6), 1-10.

[18] Khamaia, D., Boudhiaf, R., Khechekhouche, A., and Driss, Z. (2022). Illizi city sand impact on the output of a conventional solar still. *ASEAN Journal of Science and Engineering Education*, *2*(3), 267-272

[19] Khechekhouche, A., de Oliveira Siqueira, A. M., and Elsharif, N. (2022). Effect of plastic fins on a traditional solar still's efficiency. *International Journal of Energetica*, *7*(1), 23-27.

[20] Khechekhouche, A., Zine, A., Kabeel, A. E., Elmashad, Y., and Abdelgaied, M. (2023). Energy, exergy investigation of absorber multilayered composites materials of a solar still in Algeria. *Journal of Testing and Evaluation*, *51*(5), 3001-3013.

DOI: https://doi.org/10.17509/ijost.v10i3.85150
p- ISSN 2528-1410 e- ISSN 2527-8045

[21] Barkat, A., Rahal, Z., Medjdoub, K., Daoud, A., Mester, T., Chekima, H., and Bellila, A. (2024). Evaluating the impact of absorber geometry on solar still efficiency: A comparative study of square and round absorbers. *International Journal of Energetica*, *9*(1), 24-30.

[22] Suraparaju, S. K., Samykano, M., Nandavarapu, R. R., Natarajan, S. K., Muthuvairavan, G., Yadav, A., and Vasudevan, G. (2025). Innovative double-finned absorber and nanoparticle-enhanced energy storage for enhanced thermo-economic performance of solar stills. *Separation and Purification Technology*, *361*(Part 1), 131360.

[23] Chang, Z., Yang, J., Chu, Y., Hou, J., and Su, Y. (2025). Energy, exergy and economic analysis of a novel immersion tapered solar still for combination with solar concentrator. *Desalination*, *601*, 118560.

[24] Alshammari, F., Alanazi, N., Alshammari, M., Elsheikh, A. H., and Essa, F. A. (2025). Enhancing tubular solar still productivity: A novel rotational absorber, ultrasonic atomizer, and hygroscopic fabric integration. *Solar Energy Materials and Solar Cells*, *287*, 113622.

[25] Gokulnath, R., Elijah, E. S., and Bandaru, R. (2025). Performance evaluation of modified wick belt configuration in rotating wick solar stills using different wick materials. *Thermal Science and Engineering Progress*, *60*, 103457.

[26] Mohaisen, H. S., and Alhusseny, A. (2025). Enhancing productivity and cost-effectiveness of single-slope solar stills using a multi-cavity built-in condenser: Experimental and performance analysis. *Cleaner Engineering and Technology*, *2025*, 100970.

[27] Chopra, K., Sharma, M., Tyagi, V. V., Popli, S., Kothari, R., Rajamony, R. K., Mansor, M., and Pandey, A. K. (2025). Energy, exergy, economic and enviro-economic analysis of solar still with macro-encapsulated phase change material for wastewater treatment: Experimental validation study using machine learning. *Separation and Purification Technology*, *2025*, 133031.

[28] Attia, M. E. H., Kabeel, A., Moharram, N. A., El-Maghlany, W. M., and Fayed, M. (2025). Enhancing freshwater yield in conical solar stills utilizing external reflective mirrors: An experimental approach. *Solar Energy*, *288*, 113287.

[29] Işık, S. K., and El, E. (2024). Experimental investigation of distilled water production performance of conventional solar stills using $CaCl_2 \cdot 6H_2O$ phase change material reinforced with $SrCl_2 \cdot 6H_2O$ and graphene-based nanoparticles. *Case Studies in Thermal Engineering*, *62*, 105184.

[30] Sonker, V. K., Sharma, P., Ram, R., and Sarkar, A. (2025). A CFD simulation analysis of the effects of PCM and nanoparticles stored in copper cylinders inside a solar still. *Journal of Energy Storage*, *108*, 115091.

[31] Abdullah, A. S., Omara, Z. M., Alawee, W. H., Shanmugan, S., and Essa, F. A. (2025). Leveraging nanoparticles for sustainable water harvesting: A review of solar still technologies. *Results in Engineering*, *25*, 104128.

[32] Ansari, U. N., and Kushwaha, N. (2025). Exploring the influence of integrating nano-enhanced phase change material on various solar still systems productivity: A systematic literature review. *Desalination*, *609*, 118851.

DOI: https://doi.org/10.17509/ijost.v10i3.85150
p- ISSN 2528-1410 e- ISSN 2527-8045

[33] Manokar, A. M., Winston, D. P., Mondol, J. D., Sathyamurthy, R., Kabeel, A. E., and Panchal, H. (2018). Comparative study of an inclined solar panel basin solar still in passive and active mode. *Solar Energy*, *169*, 206-216.

[34] Kerans, G., Sanjaya, Y., Liliasari, L., Pamungkas, J., and Ate, G., Y. (2024). Effect of substrate and water on cultivation of Sumba seaworm (nyale) and experimental practicum design for improving critical and creative thinking skills of prospective science teacher in biology and supporting sustainable development goals (SDGs). *ASEAN Journal of Science and Engineering*, *4*(3), 383-404.

[35] Makinde, S.O., Ajani, Y.A., and Abdulrahman, M.R. (2024). Smart learning as transformative impact of technology: A paradigm for accomplishing sustainable development goals (SDGs) in education. *Indonesian Journal of Educational Research and Technology*, *4*(3), 213-224.

[36] Gemil, K.W., Na'ila, D.S., Ardila, N.Z., and Sarahah, Z.U. (2024). The relationship of vocational education skills in agribusiness processing agricultural products in achieving sustainable development goals (SDGs). *ASEAN Journal of Science and Engineering Education*, *4*(2), 181-192.

[37] Haq, M.R.I., Nurhaliza, D.V., Rahmat, L.N., and Ruchiat, R.N.A. (2024). The influence of environmentally friendly packaging on consumer interest in implementing zero waste in the food industry to meet sustainable development goals (SDGs) needs. *ASEAN Journal of Economic and Economic Education*, *3*(2), 111-116.

[38] Basnur, J., Putra, M.F.F., Jayusman, S.V.A., and Zulhilmi, Z. (2024). Sustainable packaging: Bioplastics as a low-carbon future step for the sustainable development goals (SDGs). *ASEAN Journal for Science and Engineering in Materials*, *3*(1), 51-58.

[39] Maulana, I., Asran, M.A., and Ash-Habi, R.M. (2023). Implementation of sustainable development goals (SDGs) no. 12: Responsible production and consumption by optimizing lemon commodities and community empowerment to reduce household waste. *ASEAN Journal of Community Service and Education*, *2*(2), 141-146.

[40] Nurnabila, A.T., Basnur, J., Rismayani, R., Ramadhani, S., and Zulhilmi, Z. (2023). Analysis of the application of Mediterranean diet patterns on sustainability to support the achievement of sustainable development goals (SDGs): Zero hunger, good health and well beings, responsible consumption, and production. *ASEAN Journal of Agricultural and Food Engineering*, *2*(2), 105-112.

[41] Awalussillmi, I., Febriyana, K.R., Padilah, N., and Saadah, N.A. (2023). Efforts to improve sustainable development goals (SDGs) through education on diversification of food using infographic: Animal and vegetable protein. *ASEAN Journal of Agricultural and Food Engineering*, *2*(2), 113-120.

[42] Rahmah, F.A., Nurlaela, N., Anugrah, R., and Putri, Y.A.R. (2024). Safe food treatment technology: The key to realizing the sustainable development goals (SDGs) zero hunger and optimal health. *ASEAN Journal of Agricultural and Food Engineering*, *3*(1), 57-66.

[43] Keisyafa, A., Sunarya, D.N., Aghniya, S.M., and Maula, S.P. (2024). Analysis of student's awareness of sustainable diet in reducing carbon footprint to support sustainable development goals (SDGs) 2030. *ASEAN Journal of Agricultural and Food Engineering*, *3*(1), 67-74.

DOI: https://doi.org/10.17509/ijost.v10i3.85150
p- ISSN 2528-1410 e- ISSN 2527-8045